

## **General Disclaimer**

### **One or more of the Following Statements may affect this Document**

- This document has been reproduced from the best copy furnished by the organizational source. It is being released in the interest of making available as much information as possible.
- This document may contain data, which exceeds the sheet parameters. It was furnished in this condition by the organizational source and is the best copy available.
- This document may contain tone-on-tone or color graphs, charts and/or pictures, which have been reproduced in black and white.
- This document is paginated as submitted by the original source.
- Portions of this document are not fully legible due to the historical nature of some of the material. However, it is the best reproduction available from the original submission.

(NASA-TM-83929) A COMPARISON OF THE X-RAY  
PROPERTIES OF X PER AND GAMMA CAS (NASA)  
34 p HC A03/MF A01 CSCL 03A

N82-27201

G3/89 24372  
Unclas

**NASA**

Technical Memorandum 83929

**A COMPARISON OF THE X-RAY  
PROPERTIES OF X PER AND  
 $\gamma$  CAS**

N. E. White, J. H. Swank,  
S. S. Holt and A. N. Parmar

APRIL 1982

National Aeronautics and  
Space Administration

**Goddard Space Flight Center**  
Greenbelt, Maryland 20771



A COMPARISON OF THE X-RAY PROPERTIES OF X PER AND  $\gamma$  CAS

N.E. White<sup>1</sup>, J.H. Swank, S.S. Holt  
Laboratory for High Energy Astrophysics  
NASA/Goddard Space Flight Center  
Greenbelt, Maryland 20771

and

A.N. Parmar  
Mullard Space Science Laboratory  
Holmbury St. Mary  
Dorking  
Surrey  
ENGLAND

<sup>1</sup>Also Dept. Physics & Astronomy, Univ. of Maryland

## ABSTRACT

We examine the X-ray properties of the main sequence Be stars X Per and  $\gamma$  Cas, and conclude that the latter is, like the former, a widely separated binary system containing an accreting neutron star. The X-ray spectra in the 2-20 keV band are very similar, and can be characterized by  $\sim 10$  keV thermal emission. A high energy excess in the spectrum of X Per, spectral variations across the X Per pulse and the lack of any iron emission at 6.7 keV from both  $\gamma$  Cas and X Per suggest that the emission is not truly thermal, and that we are using a simple spectral model to approximate the complex emission from the magnetic pole of an accreting neutron star. No X-ray pulsations greater than  $\sim 5\%$  and  $15\%$  semi-amplitude are detected from  $\gamma$  Cas for periods from 80 ms to 15 min and 15 min to 20 min respectively; this is in contrast to X Per's 13.9 minute X-ray pulsations with  $\sim 40\%$  semi-amplitude. Non-coherent variations in the X-ray flux of both  $\gamma$  Cas and X Per on timescales of  $\sim 10$  mins probably reflect stellar wind inhomogeneities with a typical size of  $\lesssim 1 R_0$ . The long term optical brightness variations of X Per are not directly correlated with the X-ray flux, although a gradual factor of 5 reduction in the X-ray flux of X Per between 1972 and 1980 may be related to a sharp 0.5 magnitude decline in the optical brightness in 1973. X Per pulse timings rule out orbital periods  $< 40$  days. The observed X-ray luminosities, combined with the lower limits to orbital motion, indicate mass loss rates  $> 8 \times 10^{-8} v_3^4 M_\odot \text{ yr}^{-1}$  and  $> 9 \times 10^{-8} v_3^4 M_\odot \text{ yr}^{-1}$  from X Per and  $\gamma$  Cas respectively, where  $v_3$  is the wind velocity in  $1000 \text{ km s}^{-1}$ . The mass loss rates in the plane of the X-ray source are at least an order of magnitude larger than that given by UV measurements and support earlier suggestions of a strong inclination dependence for the mass loss process from main sequence OB stars.

## I. INTRODUCTION

The detection of X-ray emission from X Per (4U0352+30) and  $\gamma$  Cas (MX0053+604) helped establish the existence of a class of low luminosity ( $< 10^{35}$  ergs  $s^{-1}$ ) X-ray sources associated with rapidly rotating main sequence Be stars (Bradt et al. 1977; Mason, White and Sanford 1976; Maraschi, Treves and van den Heuvel 1976). The 13.9 minute X-ray pulsations from X Per indicate the presence of a degenerate companion (White et al. 1976) and secular changes in the pulse period suggest that it is a neutron star (White, Mason and Sanford 1977; Mason 1977; Rappaport and Joss 1977), although an unambiguous determination of the orbital period remains elusive (Hutchings, et al. 1974; White, Mason and Sanford 1977; Becker et al. 1979).  $\gamma$  Cas (B0.5 II-V) is photometrically and spectroscopically very similar to X Per (O9.5 III-V; Moffat, Kaupt, and Schmidt-Kaler 1973), and while it has been suggested that the X-ray emission from  $\gamma$  Cas may be coronal in origin (Marlborough 1977; Cowley, Rogers and Hutchings 1976), accretion-driven models have also been considered (Marlborough, Snow, and Stettebak 1978; Rappaport and van den Heuvel 1982). We note that  $\gamma$  Cas is surrounded by a bright nebulae (Poekert and van den Bergh 1981 and refs therein). This may be either material ejected from the Be star or the remnant of a supernova that formed a neutron star (see also Ferlet et al. 1980).

There are currently ~ 12 main sequence Be stars suspected to have neutron star companions (see Rappaport and van den Heuvel 1982 for a recent review and Schwartz et al. 1981 for two new identifications). Only for the transient 4U0115+63 has its binary orbit been positively identified, with a period of 24 days (Rappaport et al. 1978). Pulse timings and quasi-periodic flare ups indicate that the remainder have orbital periods of order tens to hundreds of days (e.g. McClintock et al. 1977; White et al. 1978; Li et al. 1979; Watson,

Warwick and Ricketts 1981).

In this paper we present the first detailed X-ray observations of  $\gamma$  Cas and compare them with similar observations of X Per. It is concluded that  $\gamma$  Cas must be a binary system containing a neutron star with an orbital period  $> 40$  days. Avni and Goldman (1981) and others have pointed out that the presence of a neutron star in these non-Roche-limited binary systems can give valuable information concerning the mass loss process from OB stars in general, and we compare the UV-derived mass loss rates for X Per and  $\gamma$  Cas with those required to power the X-ray sources.

## II. OBSERVATIONS

The data come from observations made with the OSO-8, HEAO-1, HEAO-2 (Einstein) and Copernicus satellites. X Per was observed three times by OSO-8 in February of 1976, 1977, and 1978, each for  $\sim 5$  days. The results from the first two observations have been reported in Becker et al. (1979). A six hour pointed observation was made by the HEAO-1 A2<sup>+</sup> experiment on 1978

---

<sup>+</sup>The A2 experiment on HEAO-1 is a collaborative effort led by E. Boldt of GSFC and G. Garmire of CIT, with collaborators at GSFC, CIT, JPL and UCB.

---

August 22 and data from the Medium Energy Detector (MED; 2-20 keV) and High Energy Detector (HED; 2-60 keV) will be discussed here. The Einstein Solid State Spectrometer (SSS; 0.5-4.5 keV) and Monitor Proportional Counter (MPC; 1.5-10 keV) observed X Per on 1979 Feb 10. We also present extended observations of X Per made between 1972 and 1980 by the UCL/MSSL 2-8 keV detector on Copernicus. The  $\gamma$  Cas results are from a six hour HEAO-1 A2 pointed observation of 1978 August 7 and MPC/SSS Einstein observations on 1979 Jan 18 and 1979 July 17 and 18.

### III. TIME VARIABILITY

Figures 1 and 2 show parts of the Einstein MPC observations of X Per and  $\gamma$  Cas. To facilitate easy comparison, the scale of the abscissa is the same for both. Individual 13.9 min pulsations can be clearly seen in the X Per data (Figure 1) along with factor of 2 changes in the intensity from pulse to pulse.  $\gamma$  Cas (Figure 2) shows factor of 2 quasi-periodic variations on a timescale similar to that of the pulsations from X Per. However, even though the data are very suggestive of a  $\sim 20$  min periodicity, Fourier analysis does not reveal a unique period to be present in any of the three data sets, with a 3-sigma upper limit of 5% the mean flux for periods between 160 ms and 15 min, and 15% for periods between 15 and 20 min. The presence of the 97 min orbital period of the satellite, earth occultation and the limited nature of the observations prevented a reliable search for periods greater than  $\sim 20$  mins. Also shown in Figures 1 and 2 is a spectral measure obtained from a ratio of hard-to-soft detected photons. While there are significant spectral variations associated with the pulsations from X Per, both the X Per pulse-to-pulse variations and the variability from  $\gamma$  Cas are spectrally independent.

Kaitchuck et al. (1982) have reported that there is a softening of the spectrum of X Per at pulse minimum, contradicting an earlier report by Becker et al. (1979) of spectral hardening at the same pulse phase. The hardness ratio shown in Figure 1 does show a tendency for a spectral softening at pulse minimum. In Figure 3 we show the average pulse profile in two energy bands, and the ratio of those two bands for each of the OSO-8 and HEAO-1 MED + HED observations. The latter was simultaneous with the observations of Kaitchuck et al. In all three OSO-8 profiles there is, for  $\sim 10\%$  of the cycle, a hardening of the spectrum which terminates at pulse minimum. But the MED +

HED profile only shows a softening at pulse minimum, with no evidence for the hard pulse. The softening is not at the same phase as the hardening seen in the OSO-8 data, but immediately follows it. A more careful re-examination of the OSO-8 profiles does, in addition, show a slight softening at the same phase where it is seen by HEAO-1.

To investigate this further, the Feb 76 OSO-8 PHA spectra taken during the hard ( $\phi \sim 0.86-0.96$ ) and soft ( $\phi \sim 0.96-0.09$ ) pulse phases were divided by the spectrum at the pulse peak ( $\phi \sim 0.5$ ), and normalized to unity. These are shown in Figure 4, where it can be seen that the hardening only occurs above 10 keV, while the softening is limited to below 5 keV. The HEAO-1 MED and OSO-8 detectors are not identical; in particular, the combined response of the HEAO-1 A2 MED + HED biases the centroid of the chosen energy band to lower energies than that of OSO-8. The HEAO-1 HED, however, has a response very similar to the OSO-8 detector, and with the HED data alone the hard pulse at  $\phi \sim 0.9$  is again evident (Figure 4).

#### IV. THE X-RAY SPECTRA OF X PER AND $\gamma$ CAS

The HEAO-1 A2 Medium Energy Detector (MED; 2-25 keV) and High energy Detector (HED; 2-60 keV) observed both sources with 64 channels of PHA resolution. Acceptable fits were obtained for two standard spectral models, with results given in Table 1 and 2 for X Per and  $\gamma$  Cas, respectively.

Becker et al. (1979) and White et al. (1976) found the spectrum of X Per in the 2-20 keV band to be consistent with thermal bremsstrahlung with a temperature of  $\sim 12$  keV. The thermal fits to the MED and HED data from HEAO-1 find temperatures similar to those found previously, but the reduced  $\chi^2$  for the HED of 2.8 is formally unacceptable. In contrast, a power law model with  $\alpha \sim 1$  gives an acceptable fit for the HED data but not for the MED data (Table 1). The discrepancy between the two detectors suggests the presence of

a high energy excess above that predicted by thermal bremsstrahlung, that is only evident with the extended energy range of the HED. A similar result has been independently found by Worrall et al. (1981) from combining the HEAO-1 A4 high energy data with the HEAO-1 A2 results presented here. A two component blackbody plus power law model or a thermal plus power law model each give a reduced  $\chi^2$  of  $\sim 1$  in both detectors, which are summarized in Table 1. The total luminosity in the 0.5-60 keV band was  $4 \times 10^{33}$  erg s<sup>-1</sup>, for a distance of 350 pc (Brucato and Kristian 1972).

There is no evidence for an iron line at  $\sim 6.7$  keV with a 3 sigma upper limit to the equivalent width (EW) for a narrow line of 150 eV. This further demonstrates that the X-ray spectrum of X Per is not truly thermal, as an optically thin plasma in collisional equilibrium at a temperature of 9 keV should give an  $\sim 800$  eV EW iron line. The spectral variations across the pulse indicate that a two component model may not be physically meaningful. During the region of pulse hardening the soft component is no longer required and a single power law with  $\alpha \sim 1$  gives an acceptable fit to the whole spectrum. This is not caused by the eclipse of the soft component; rather Figure 4 shows that the shape of the overall spectrum above 10 keV has changed. Likewise during the pulse softening the hard component does not change, only the spectral shape below  $\sim 5$  keV. This suggests that the two component model is only a convenient representation of a spectrum that below  $\sim 20$  keV can be approximated by an exponential form with  $kT \sim 10$  keV, and above by a power law with  $\alpha \sim 1$ .

The overall spectrum of X Per is softer than that normally associated with X-ray pulsars. The more luminous X-ray pulsars are characterized by a flat ( $\alpha \sim 0$ ) power law spectra up to 20 or 30 keV, above which their intensity falls off sharply (White, Swank and Holt 1982 and refs. therein). This

difference may be related to the low luminosity of this source of  $\sim 10^{33}$  ergs  $s^{-1}$ , as compared to  $> 10^{35}$  ergs  $s^{-1}$  for typical X-ray pulsars.

The 2-60 keV HEAO-1 A2 spectra of  $\gamma$  Cas are equally well fit by either a power law with  $\alpha \sim 1$ , or a thermal bremsstrahlung with  $kT \sim 14$  keV. However the SSS spectrum in the 0.5-4.5 keV band is consistent with only the thermal fit found by HEAO-1 A2. During August 1978  $\gamma$  Cas was fainter than X Per and the HED observation would not have been sensitive to the high energy excess seen from X Per. The inclusion of a second component in the HED data did slightly improve the fit, but was not formally required. There was no evidence for any iron emission at  $\sim 6.7$  keV greater than an EW of  $\sim 200$  eV. The 0.5-60 keV luminosity of  $\gamma$  Cas is  $1 \times 10^{33}$  ergs  $s^{-1}$  for a distance of 300 pc (Moffat et al. 1973). When the different energy bands are taken into account, this is similar to that seen previously (cf. Peters 1982). In Figure 5 we show and compare the deconvolved spectra of both  $\gamma$  Cas and X Per.

The lower bandpass of the SSS provides a determination of interstellar absorption that is relatively insensitive to uncertainties in the continuum. The column densities measured by the SSS are  $(2.2 \pm 0.7) \times 10^{21}$  H  $cm^{-2}$  to X Per and  $(1.6 \pm 0.7) \times 10^{21}$  H  $cm^{-2}$  to  $\gamma$  Cas for a thermal spectrum with  $kT \sim 10$  keV. The order-of-magnitude more absorption required by the MED and HED fits (Table 1) is probably a result of the inadequacy of the continuum model over the larger bandpass of these instruments. The amount and nature of the material in the line of sight to X Per has been thoroughly discussed by Mason et al. (1976) and the SSS measurements agree well with these results. The reddening of  $\gamma$  Cas is 0.05 (Moffat et al. 1973) and predicts an  $N_H$  of  $3 \times 10^{20}$  H  $cm^{-2}$  (Gorenstein 1975; Ryter, Cesarsky and Audouze 1975), which is a factor of 5 below that observed. This might indicate some local attenuation of the X-ray source. We note that X Per has been seen to undergo a transient factor

of 2 increase in absorption (White et al. 1976).

#### V. THE LONG-TERM X-RAY AND OPTICAL BEHAVIOR OF X PER

The UCL/MSSL 2-8 keV detector on Copernicus has regularly monitored the X-ray flux from X Per throughout the operational lifetime of the satellite (1972-1980), and the background subtracted count rate is shown in Figure 6. A factor of 5 decrease in the flux is apparent over the eight years of observations. Regular calibrations using the Crab Nebula ensured that this is not an instrumental effect. Also given in Figure 6 is the corresponding V magnitude. In 1973 the star dimmed by half a magnitude to  $\sim 6.8$ , the faintest it has been since 1907 (Margon, Bowyer and Penegor 1976; Gottlieb, Wright and Liller 1975) and, apart from a short lived recovery in late 1977/early 1978 (Dorren and Guinan 1980), it has remained relatively dim since then. The more gradual decrease in X-ray luminosity over the same interval may be related to the optical variations, although there is no increase in X-ray flux associated with the optical brightening in 1977/1978. There was no significant change in the pulse amplitude associated with the decrease in the X-ray luminosity.

The history of the pulse period is also shown in Figure 6. This includes three new measurements of the period; two by Copernicus and one by OSO-8. All the current accurate heliocentric pulse period measurements are given in Table 3. After 1978 the X-ray source became too weak to allow a reliable estimate of the period to be made by Copernicus. The length of the observations by HEAO-1 A2 and Einstein were too short to give useful measurements of the period. The overall secular decrease in the period reported by White, Mason and Sanford (1977) is apparent, although from mid-1974 to 1978 there has been little overall change in the period. This may be related to the decrease in X-ray luminosity over the same interval reflecting a reduced mass transfer onto the neutron star, with a corresponding reduction in the accretion torque.

Hutchings et al. (1974,1975) have reported evidence for a 581 day orbital period in some of the absorption and emission lines of X Per, although the mass function derived requires the X-ray source to be 20-40  $M_{\odot}$ , much higher than that of a neutron star. The residuals from the secular decrease in the period may suggest a complementary modulation of the pulse period (White, Mason and Sanford 1977), although we note that this result is dependent on the assumption of a constant secular decrease in pulse period, which may be in doubt given the fluctuations in X-ray luminosity. The three additional period measurements do not extend the baseline sufficiently to comment further on this. The past problems associated with deconvolving orbital period variations from those caused by the accretion process (e.g. Li et al. 1979), suggest that this technique will require hundreds of days of monitoring the pulse period to obtain a definitive measure of the orbital period. In fact, to emphasize this point, we find that the pulse phases obtained over the last three years, when the average pulse period was relatively stable, give some evidence for a ~ 250 day modulation. Unfortunately the coverage is very patchy, and it is necessary to make arbitrary assumptions concerning the pulse phasing from one observation to the next.

We can, however, test for binary periods in the range 1-40 days. The longest intervals of phase measurements where the pulse phasing is certain last ~ 20 days and exclude the region of the  $a_x \sin i$  versus orbital period diagram shown in Figure 7. For comparison the locus is shown for a total system mass equal to 20  $M_{\odot}$  and  $i=90^{\circ}$ . Orbital periods less than one day are unlikely because a main sequence B0 star will be at or beyond its Roche radius and tidal distortions would probably have been detected (Mazeh and Brosch 1981). As already noted by Becker et al. (1979), there was no evidence in the OSO-8 observations for the 11 or 22 hr variations seen by White et al.

(1976). The emission lines of X Per (and  $\gamma$  Cas) show the characteristic double peak of a Be star viewed reasonably close to its equatorial plane ( $i > 45^\circ$ ). Unless there is a fortuitous misalignment of the orbital and rotation planes it is very probable that the orbital period is  $> 40$  days.

#### VI. THE BINARY NATURE OF $\gamma$ CAS

There can be little doubt that the X-ray emission associated with  $\gamma$  Cas is produced by accretion onto a neutron star. The  $\sim 10$  keV thermal spectrum and erratic spectrally independent variations on a timescale of  $\sim 10$ -20 mins are very similar to the properties of the X-ray emission associated with the X-ray pulsar in the X Per system. The X-ray spectrum does not in any way resemble the coronal emission seen from OB stars observed with the SSS. For example, the spectra of 3 Orion supergiants are characterized by 0.25-0.5 keV thermal emission with at least two orders of magnitude less flux at 2 keV than that seen from  $\gamma$  Cas (Cassinelli and Swank 1982). A 14 keV thermal interpretation of the emission from  $\gamma$  Cas predicts an iron line at 6.7 keV with an EW about twice the observed upper limit. This suggests that, as is probably the case for X Per, the exponential model is only a convenient spectral representation of a more complex underlying emission process (see Section IV). Pallavicini et al. (1981) have shown that the observed X-ray luminosity from all luminosity classes of stars earlier than A is proportional to the bolometric luminosity ( $L_x \sim 10^{-7} L_{bol}$ ). This predicts for  $\gamma$  Cas an X-ray luminosity 30 times less than that observed. Therefore we conclude that  $\gamma$  Cas is part of a binary system and that, by analogy with X Per, the secondary is an accreting neutron star. The lack of any X-ray pulsations from  $\gamma$  Cas could be caused by three possibilities: the rotation period is  $> 20$  mins; the magnetic and rotation axes of the neutron star are aligned such that the amplitude of the modulation is below our limits; or the polar caps

cover a substantial fraction of the surface area of the neutron star. Arons and Lea (1980) have proposed that for spherical accretion the size of the polar cap region increases with decreasing  $L_x$ , so that when  $L_x < 10^{35}$  erg  $s^{-1}$  the whole hemisphere of the star could be covered. The fact that X-ray pulsations are detected from X Per, however, suggests that one of the other two possibilities might be more appropriate in this case.

### VII. MASS LOSS RATES

Cowley, Rogers and Hutchings (1976) have examined spectroscopic data from  $\gamma$  Cas, and they find that the orbital period of a  $2 M_\odot$  secondary must be  $> 100$  days. Figure 7 indicates that the orbital period of X Per is  $> 40$  days. There is no evidence for any tidal distortion of either  $\gamma$  Cas or X Per, so the material that eventually falls onto the neutron star must be accreted from the stellar wind of the primary. In such cases, the presence of the neutron star should have no effect on the mass loss rate from the primary. A  $1.4 M_\odot$  neutron star will capture all the material within a radius of  $4 \times 10^{10} M_{1.4} v_3^{-2}$  cm, where  $v_3$  is the velocity of the wind relative to the neutron star in units of  $1000 \text{ km s}^{-1}$  and  $M_{1.4}$  is the X-ray source mass in units of  $1.4 M_\odot$  (Davidson and Ostriker 1973; Bondi and Hoyle 1944). This assumes that the Alfvén radius is less than the capture radius, which will be true for wind velocities less than  $\sim 3000 \text{ km s}^{-1}$ . By considering the capture radius, Kepler's third law, and the gravitational potential energy released by the material falling onto the degenerate star and assuming spherical symmetry, the rate of mass loss from the primary in the orbital plane is given by

$$\dot{M} = 2 \times 10^{-11} \cdot L_{33} \cdot \left[ \frac{R_x}{10 \text{ km}} \right] \cdot M_{1.4}^{-3} \cdot v_3^4 \left[ \frac{M_T}{M_\odot} \right]^{2/3} \cdot P_d^{4/3} \cdot M_\odot \text{ yr}^{-1}$$

where  $L_{33}$  is the X-ray luminosity in  $\text{erg s}^{-1}$ ,  $R_x$  the radius of the degenerate star,  $M_T$  is the total system mass ( $\sim 20 M_\odot$ ), and  $P_d$  is the orbital period in days. This equation is strongly dependent on the velocity of the wind; nonetheless a useful comparison with other estimates of the mass loss from these stars can be made.

The velocity law of the material leaving the star is somewhat uncertain. The theoretical radiatively driven wind law of Castor, Abbott and Klein (1975, CAK) gives a wind velocity that is 90% of the terminal value  $V_T$  at  $5 R_*$ , where  $R_*$  is the distance from the star in stellar radii. However Barlow and Cohen (1977, BC) measure for P Cygni a much more gradual velocity law where 90% of  $V_T$  is not achieved until  $\sim 40 R_*$ . For the given lower limits to the orbital periods the binary separations of X Per and  $\gamma$  Cas are respectively  $> 20 R_*$  and  $> 33 R_*$  (assuming  $R_* = 7.4 R_\odot$  and  $M_T \sim 20 M_\odot$ ), such that  $v > 0.80 V_T$  and  $v > 0.88 V_T$  for the BC law. In systems such as X Per and  $\gamma$  Cas, well-saturated P Cygni profiles are not seen and it is difficult to directly estimate  $V_T$ . Hammerschlag-Hensberge et al. (1980) find velocities up to  $1000 \text{ km s}^{-1}$  and  $800 \text{ km s}^{-1}$  for X Per and  $\gamma$  Cas, although subsequently Henrichs and Hammerschlag-Hensberge (1980) also saw narrow absorption cores from  $\gamma$  Cas indicating  $V_T > 1800 \text{ km s}^{-1}$ . Abbott (1978) has shown that for many OB stars  $V_T$  is approximately three times the escape velocity  $V_E$  (which is  $\sim 1000 \text{ km s}^{-1}$  for a main sequence B0 star). The star  $\tau$  Sco (B0V) has an observed maximum velocity of  $\sim 2000 \text{ km s}^{-1}$  which, because a sharp violet edge to the absorption line is not seen, may only be two thirds of the true terminal velocity (Abbott 1978). We will conservatively assume that  $V_T$  for both X Per and  $\gamma$  Cas is  $1000 \text{ km s}^{-1}$ , but the reader should bear in mind that

they may be up to three times larger (corresponding to a factor 80 higher  $\dot{M}_x$ ).

From the observed X-ray luminosities and the lower limits to the orbital periods we can infer a minimum mass loss rate of  $> 8 \times 10^{-8} v_3^4$  and  $> 9 \times 10^{-8} v_3^4 M_\odot \text{ yr}^{-1}$  for X Per and  $\gamma$  Cas respectively, assuming the X-ray luminosities measured by HEAO-1 A2 in August 1978. Because it is likely that the orbital periods are of order several hundred days, we have also calculated  $\dot{M}$  for an arbitrary orbital period of 250 days. These are  $9 \times 10^{-7} v_3^4 M_\odot \text{ yr}^{-1}$  and  $3 \times 10^{-7} v_3^4 M_\odot \text{ yr}^{-1}$  for X Per and  $\gamma$  Cas. If the terminal velocity of  $\gamma$  Cas is in excess of  $1800 \text{ km s}^{-1}$ , then mass loss rates as high as  $10^{-5} M_\odot \text{ yr}^{-1}$  are required to power the X-ray source.

The radiation absorbed and emitted by the stellar wind of early stars has been modelled by various workers to deduce the mass loss rates. Four techniques have been developed that each utilize a different waveband: the UV (e.g. Gathier, Lamers, and Snow 1981), the optical (e.g. Conti and Frost 1977), the IR (Barlow and Cohen 1977) and the radio (Abbott et al. 1980). The first three techniques involve processes that occur within a few stellar radii, and the results are critically dependent on the wind model. Only mass loss estimates from the UV have been made for  $\gamma$  Cas and X Per and these (which were derived assuming the CAK velocity law) are summarized in Table 4 along with our X-ray estimates. For X Per  $\dot{M}_{UV}$  ranges from  $1 \times 10^{-9}$  to  $1 \times 10^{-8} M_\odot \text{ yr}^{-1}$  and for  $\gamma$  Cas from  $6 \times 10^{-11}$  to  $7 \times 10^{-9} M_\odot \text{ yr}^{-1}$ . All these estimates are at least an order of magnitude below that required to power the X-ray source. This cannot be caused by fortuitous long term changes in the wind because some of the IUE measurements were made within a month of the HEAO-1 A2 observations. The discrepancy might indicate that the velocity of the wind in the vicinity of the X-ray source has not reached its terminal value and is

lower than that predicted by the BC velocity law. However the UV mass loss rates are sensitive to changes in the velocity law and would also have to be revised downwards accordingly (cf. Table 4). The photoionization of the wind around the X-ray source will not penetrate close enough to the mass-losing star to have any significant disrupting effect on the acceleration process.

It is generally agreed that for many OB stars  $\dot{M}$  is a function of the stellar luminosity of the star  $L_S$ , supporting the hypothesis that the winds are radiatively driven. Because the radio emission originates from tens to hundreds of stellar radii, these measurements are relatively model-independent and have probably given the most reliable estimates to date. The only main sequence star for which both radio and UV measurements have been made is 9 Sge, an O4 star with a  $v \sin i$  of  $168 \text{ km s}^{-1}$  (compared to  $300\text{-}400 \text{ km s}^{-1}$  for  $\gamma$  Cas and X Per). It is notable that in this case the radio gives a mass loss rate of  $3 \times 10^{-5} M_{\odot} \text{ yr}^{-1}$ , 30 times greater than UV and optical measurements (Abbott et al. 1980). However for supergiants the agreement is much better and the radio measurements have been used to calibrate the estimates from other wavebands giving an empirical relation between  $\dot{M}$  and the stellar luminosity. Snow (1982) has found that this relation may extrapolate to dwarf stars like X Per and  $\gamma$  Cas and that the 9 Sge result is anomalous. The relation most recently derived by Abbott (1982) predicts a mass loss rate of  $\sim 10^{-8} M_{\odot} \text{ yr}^{-1}$ , consistent with the UV estimates but still far below the X-ray values, suggesting that for these stars a rotational dependence should be included in any empirical relation. The nature of the factor 2 variations in the optical luminosity of X Per are not understood and the lack of rapid response from the X-ray source further indicates that the mass loss rate in the orbital plane is insensitive to  $L_S$ . The  $\sim 10$  min erratic variations in the X-ray flux may reflect the inhomogeneities in the wind seen by Henrichs

and Hammerschlag-Hensberge (1980). This gives a characteristic size of  $\sim 1 R_{\odot}$  which, it is interesting to note, is similar to the size of the capture radius and may suggest that smaller scale inhomogeneities are smeared out by the accretion process.

The discrepancy between the X-ray and the UV measurements must be considered in the light of the fact that we are sampling the mass loss in different directions. If there is any inclination dependence in the mass loss rate or terminal velocity of the wind caused by the rotation of the star, then the simple assumption of spherical symmetry must be abandoned. In fact many authors have speculated that such effects are important (e.g. Marlborough and Zamir 1975; Snow and Marlborough 1976; Parkes, Murdin and Mason 1980; Furenlid and Young 1980) and that they might explain the high  $\dot{M}$  estimate for 9 Sge from the radio observation (Abbott et al. 1980). X Per and  $\gamma$  Cas are both rotating close to break up velocity and calculations by Castor (1978) suggest that the rotation of the B star will lower the terminal velocity at the equator because the centrifugal force reduces the effective escape velocity ( $V_T = 3 V_E$ ). To account for the observed X-ray luminosities the terminal velocity in the orbital plane must be  $< 500 \text{ km s}^{-1}$ , at least a factor 2 below that observed. Because the X-ray luminosity is so sensitive to velocity, the orbital and rotation planes must be very closely aligned to avoid huge variations in the X-ray luminosity with orbital phase. Conversely, if there is any misalignment this might provide a natural explanation for some of the periodic transient outbursts seen from other members of this class (Johnston et al. 1979; Watson, Warwick and Ricketts 1981; Rappaport and van den Heuvel 1982), although this cannot account for outbursts like that from 4U0115+63 which repeat on timescales much greater than the orbital period, and are more likely caused by mass loss episodes from the equatorial regions of the primary (Parkes, Murdin

and Mason 1980; Rappaport and van den Heuvel 1982).

#### VIII. CONCLUSION

The large  $\gg 10^{-4} M_{\odot} \text{ yr}^{-1}$  mass loss rates required to power the X-ray sources if the compact objects were white dwarfs ( $R_x = 10^4 \text{ km}$ ) are many orders of magnitude greater than even the highest estimates for X Per and  $\gamma$  Cas. This provides independent confirmation that the compact objects in these systems are neutron stars. While the observed mass loss rates are in the realm of that required to power the X-ray emission from a neutron star, the X-ray measurements find rates at least an order of magnitude above UV estimates and support earlier suggestions that the mass loss from rapidly rotating main sequence OB stars is inclination dependent, with mass loss rates in the orbital plane at least one order of magnitude higher, or terminal velocities at least a factor of 2 lower, than indicated by UV measurements.

#### ACKNOWLEDGMENTS

We thank: Stuart Mufson for an advanced copy of the HEAO-1 A1 results; our colleagues at GSFC for their indirect contributions to this work; and Diana Worrell, David Abbott, and Saul Rappaport for critically reading an earlier manuscript. Peter Sanford and Maureen Locke provided invaluable advice and assistance throughout the planning of the Copernicus observations.

## REFERENCES

- Abbott, D.C. 1978, Ap. J. 225, 893.
- Abbott, D.C. 1982, Ap. J., in press.
- Abbott, D.C., Biegging, J.M., Churchwell, E., and Cassinelli, J.P. 1980, Ap. J. 238, 196.
- Arons, J. and Lea, S.M. 1980, Ap. J. 235, 1016.
- Avni, Y. and Goldman, I. 1981, Astr. Ap. 102, 12.
- Barlow, M.J. and Cohen, M. 1977, Ap. J. 213, 737 (BC).
- Becker, R.H., Boldt, E.A., Holt, S.S., Pravdo, S.H., Robinson-Saba, J., Serlemitsos, P.J. and Swank, J.H. 1979, Ap. J. 227, L21.
- Bernacca, P.L. and Bianchi, L. 1981, Astr. Ap. 94, 345.
- Bondi, H. and Hoyle, F. 1944, MNRAS 104, 273.
- Bradt, H.V. et al. 1977, Nature 269, 21.
- Brucato, R.J. and Kristian, J. 1972, Ap. J. 173, L105.
- Cassinelli, J.P. and Swank, J.H. 1982, in preparation.
- Castor, J.I. 1978, IAU Symp No. 83, 175.
- Castor, J.I., Abbott, D.C., and Klein, R.I. 1975, Ap. J. 195, 157 (CAK).
- Conti, P.S. and Frost, S.A. 1977, Ap. J. 212, 728.
- Cowley, A.P., Rogers, L., and Hutchings, J.B. 1976, P.A.S.P. 88, 911.
- Davidson, K. and Ostriker, J.P. 1973, Ap. J. 179, 585.
- Dorren, J.D. and Guinan, E.F. 1980, IAU Symp., 361.
- Ferlet, R., Vidal-Madjar, A., Laurent, C., and York, D.G. 1980, Ap. J. 242, 576.
- Furenlid, I. and Young, A. 1980, Ap. J. 240, L59.
- Gathier, R., Lamers, M.J. and Snow, T.P. 1981, Ap. J. 247, 173.
- Gorenstein, P. 1975, Ap. J. 198, 95.

- Gottlieb, E.W., Wright, E.L., and Liller, W. 1975, Ap. J. 202, L13.
- Hammerschlag-Hensberge, G. et al. 1980, Astr. Ap. 85, 119.
- Henrichs, M.F., and Hammerschlag-Hersberge, G. 1980, talk presented at 2nd European IUE Conference: Tubergen.
- Hutchings, J.B., Cowley, A.P., Crampton, D., and Redman, R.O. 1974, Ap. J. 191, L101.
- Hutchings, J.B., Crampton, D., and Redman, R.O. 1975, Ap. J. 170, 313.
- Johnston, M., Bradt, H.V., Doxsey, R.E., Griffeths, R.E., Schwartz, D.A., and Schwarz, J. 1979, Ap. J. 230, 611.
- Kaitchuck, R.H., Mufson, S.L., Meekins, J.F., Wood, K.S., and Yentis, D.J. 1982, preprint.
- Li, F., Rappaport, S., Clark, G.W., and Jernigan, J.G. 1979, Ap. J. 228, 893.
- Maraschi, L., Treves, A., and van den Heuvel, E.P.J. 1976, Nature 259, 292.
- Margon, B., Bowyer, S. and Penegor, G. 1976, MNRAS 176, 217.
- Marlborough, J.M. 1977, P.A.S.P. 89, 122.
- Marlborough, J.M., Snow, T.P., and Slettebak, A. 1978, Ap. J. 224, 157.
- Marlborough, J.M. and Zamir, M. 1975, Ap. J. 195, 145.
- Mason, K.O. 1977, MNRAS 178, 81p.
- Mason, K.O., White, N.E., and Sanford, P.W. 1976, Nature 260, 690.
- Mason, K.O., White, N.E., Sanford, P.W., Hawkins, F.J., Drake, J.F., and York, D.G. 1976, MNRAS 176, 193.
- Mazeh, I. and Broseh, N. 1981, Astr. Ap. 95, 3.
- McClintock, J., Rappaport, S., Nugent, J., and Li, F. 1977, Ap. J. 216, L15.
- Moffat, A.F.J., Haupt, W., and Schmidt-Kaler, Th. 1973, Astr. Ap. 23, 433.
- Pallavicini, R., Golub, L., Rosner, R., Vaiana, G.S., Ayres, T., and Linsky, J.L. 1981, Ap. J. 248, 279.
- Parkes, G.E., Murdin, P.G., and Mason, K.O. 1980, MNRAS 190, 537.

- Persi, P., Viotti, R., and Ferrari-Toniolo, M. 1977, MNRAS 181, 685.
- Peters, G.P., 1982 P.A.S.P. 94, 157.
- Poeckert, R. and van den Bergh 1981, P.A.S.P. 93, 703.
- Rappaport, S. and Joss, P.C. 1977, Nature 266, 683.
- Rappaport, S., Clark, G.W., Cominsky, L., Joss, P.G. and Li, F.K. 1978, Ap. J. 224, L1.
- Rappaport, S. and van den Heuvel, E.P.J. 1981, IAU Symp. 98, 327.
- Ryter, C., Cersarsky, C.J., and Audouze, J. 1975, Ap. J. 198, 103.
- Schwartz, D.A. et al. 1981, B.A.A.S. 13, 834.
- Snow, T.P. 1981, Ap. J. 251, 139.
- Snow, T.P. 1982, Ap. J. 253, L39.
- Snow, T.P. and Marlborough, J.M. 1976, Ap. J. 203, L87.
- Watson, M.G., Warwick, R.S., and Ricketts, M.J. 1981, MNRAS 195, 197.
- White, N.E., Mason, K.O., Sanford, P.W., and Murdin, P. 1976, MNRAS 176, 201.
- White, N.E., Mason, K.O., and Sanford, P.W. 1977, Nature 267, 229.
- White, N.E., Parkes, G.E., Sanford, P.W., Mason, K.O., and Murdin, P.G. 1978, Nature 274, 664.
- White, N.E., Swank, J.H., and Holt, S.S. 1982, in preparation.
- Worrall, D.M., Knight, F.K., Nolan, P.L., Rothschild, R.E., Levine, A.M., Primini, F.A., and Lewin, W.H.G. 1981, Ap. J. 247, L31.

ORIGINAL PAGE IS  
OF POOR QUALITY

TABLE 1: X PER SPECTRAL FITS

	THERMAL				POWER LAW			
	N	kT	$N_H$	$\chi^2/\text{dof}$	N	$\alpha$	$N_H$	$\chi^2/\text{dof}$
MED	0.024	8.6	$1.2 \times 10^{22}$	24/35	0.013	1.2	$2.5 \times 10^{22}$	58/35
HED	0.019	10.3	$1.6 \times 10^{22}$	62/22	0.016	1.3	$4.5 \times 10^{22}$	26/22

<u>THERMAL + POWER LAW</u>							
	$N_T$	kT	$N_p$	$\alpha$	$N_H$	$\chi^2/\text{dof}$	
MED	0.025	7.1	0.0022	0.0 <sup>a</sup>	$1.3 \times 10^{22}$	29/33	
HED	0.025	6.7	0.0027	0.08	$2.5 \times 10^{22}$	33/20	

<u>BLACKBODY + POWER LAW</u>						
	$N_B$	kT	$N_p$	$\alpha$	$N_H$	$\chi^2/\text{dof}$
MED	0.0014	1.58	0.067	1.1	$1.8 \times 10^{22}$	28/33
HED	0.0013	1.35	0.079	1.0	$2.9 \times 10^{22}$	34/20

kT in keV

 $N_H$  in  $\text{H cm}^{-2}$ 

$\frac{dn}{dE}$  in  $N f(E)$  where  $f(E) = g_f(E) \exp(-E/kT)/E$ ;  
 $E^{-(\alpha+1)}$ ;  $E^2/[\exp(E/kT)-1]$  for thermal, power law

and blackbody models respectively, and  $g_f(E)$  is the Gaunt factor.

TABLE 2: γ CAS SPECTRAL FITS<sup>a</sup>

	<u>MED</u>	<u>HED</u>
THERMAL:		
$N_T$	0.005	0.005
$kT$ (keV)	$15.3 \pm 0.6$	$13.3 \pm 1.0$
$N_H$ ( $H \text{ cm}^{-2}$ )	$< 5.0 \times 10^{21}$	$< 1.0 \times 10^{22}$
$\chi^2/\text{dof}$	57/35	31/22
POWER LAW:		
$N_p$	0.02	0.03
$\alpha$	$0.75 \pm 0.10$	$1.06 \pm 0.06$
$N_H$ ( $H \text{ cm}^{-2}$ )	$< 5.0 \times 10^{21}$	$(3.0 \pm 1.0) \times 10^{22}$
$\chi^2/\text{dof}$	47/35	53/22

<sup>a</sup>See Table 1 for models

TABLE 3: THE HELIOCENTRIC PULSE PERIOD OF X PER

<u>Julian Day No (24+)</u>	<u>P (mins)</u>	<u>Satellite</u>
41620	13.9330 + 0.0038	0AO a
41674	13.9302 ± 0.0049	0AO a
42082	13.9315 ± 0.0019	0AO a
42427	13.9212 ± 0.0010	0AO a
42822	13.9229 ± 0.0015	0AO a
42832	13.9228 ± 0.0008	0SO b
43040	13.9188 ± 0.0011	0AO a
43161	13.92097 ± 0.00070	0AO a
43184	13.9196 ± 0.0011	0AO a
43200	13.9195 ± 0.0008	0SO b
43414	13.9211 ± 0.0004	0AO c
43532	13.9195 ± 0.0006	0AO c
43567	13.9213 ± 0.0013	0SO c

---

<sup>a</sup>from White, Mason and Sanford (1977)

<sup>b</sup>from Becker et al. (1979)

<sup>c</sup>this work

TABLE 4: MASS LOSS RATES ( $M_{\odot} \text{ yr}^{-1}$ )

		X Per	$\gamma$ Cas
X-ray	lower limit	$> 8 \times 10^{-8} v_3^4$	$> 9 \times 10^{-8} v_3^4$
	$P_{\text{orb}} = 250$ days	$9 \times 10^{-7} v_3^4$	$3 \times 10^{-7} v_3^4$
UV <sup>a</sup>	Hamerschlag-Hensberge et al. (1983)	$1 \times 10^{-8} (1000)$	$7 \times 10^{-9} (800)$
	Bernacca and Bianchi (1981)	$2 \times 10^{-9} (650)$	-----
	Snow (1981)	-----	$6 \times 10^{-11} (400)$
Empirical	Abbott (1982)	$\sim 5 \times 10^{-9}$	$\sim 5 \times 10^{-9}$

---

<sup>a</sup>The terminal velocity ( $\text{km s}^{-1}$ ) assumed in the modelling is given in parentheses.

## FIGURE CAPTIONS

Figure 1 - The background subtracted flux of X Per seen by the MPC on Einstein in the 1.5 - 10 keV band and the hardness ratio obtained by dividing the 4-10 keV band by the 1.5-4.0 keV band. The time axis is calibrated in terms of the number of cycles of the 13.92 min pulsations.

Figure 2 - The background subtracted flux of  $\gamma$  Cas seen by the Einstein MPC. The scale of the abscissa is identical to that of Figure 1.

Figure 3 - The X Per pulse profile on four separate occasions in two energy bands, plus the ratio of the two bands. The OSO-8 data came from a Xenon filled proportional counter. The HEAO-1 A2 data came from the combined data from Argon/Methane and Xenon proportional counters.

Figure 4 - Left: The ratio of the PHA during the spectral variations seen from X Per of  $\phi_p \sim 0.86-0.96$  (hard pulse) and  $\phi_p \sim 0.96-0.09$  (soft pulse) to that of  $\phi_p \sim 0.5$  (pulse peak), normalized to unity. These data are taken from the Feb 1976 OSO-8 observation. Right: The pulse profile in two energy bands, plus the ratio of the two bands obtained by the HEAO-1 HED (a Xenon filled proportional counter) in two energy bands, plus the ratio of the two bands.

Figure 5 - The deconvolved HEAO-1 A2 spectra of X Per and  $\gamma$  Cas.

Figure 6 - The long term behavior of X Per. The x-ray data are averaged over 30 days and come from the Copernicus 2-8 keV detector where 1 ct/64 s =

$0.4 \times 10^{-10} \text{ erg cm}^{-2} \text{ s}^{-1}$  for a Crab like spectrum. The HEAO-1 A2 observation was made ~ 10 days prior to the Copernicus observation in Sept. 1978. During the former X Per was still at an average level comparable to that seen by Copernicus at the start of 1978. Consequently a factor of 2 decrease occurred within 10 days. During the Einstein observations the flux was similar to that seen by Copernicus in late 1978/1979 and at this time X Per and  $\gamma$  Cas were at a similar apparent brightness. The pulse period in minutes comes from all the available measurements made by Copernicus and OSO 8 (Table 3). After 1978 the source was too weak to allow a reliable estimate of the period. The V magnitudes come from Mazeh and Brosch (1981), Dorren and Guinan (1980) and Persi, Viotti and Ferrari-Toniolo (1977).

Figure 7 - The lower limit of  $a_x \sin i$  vs the orbital period obtained from the lack of any variation in the X Per pulse phase as measured by OSO-8 and Copernicus in Feb 1976.

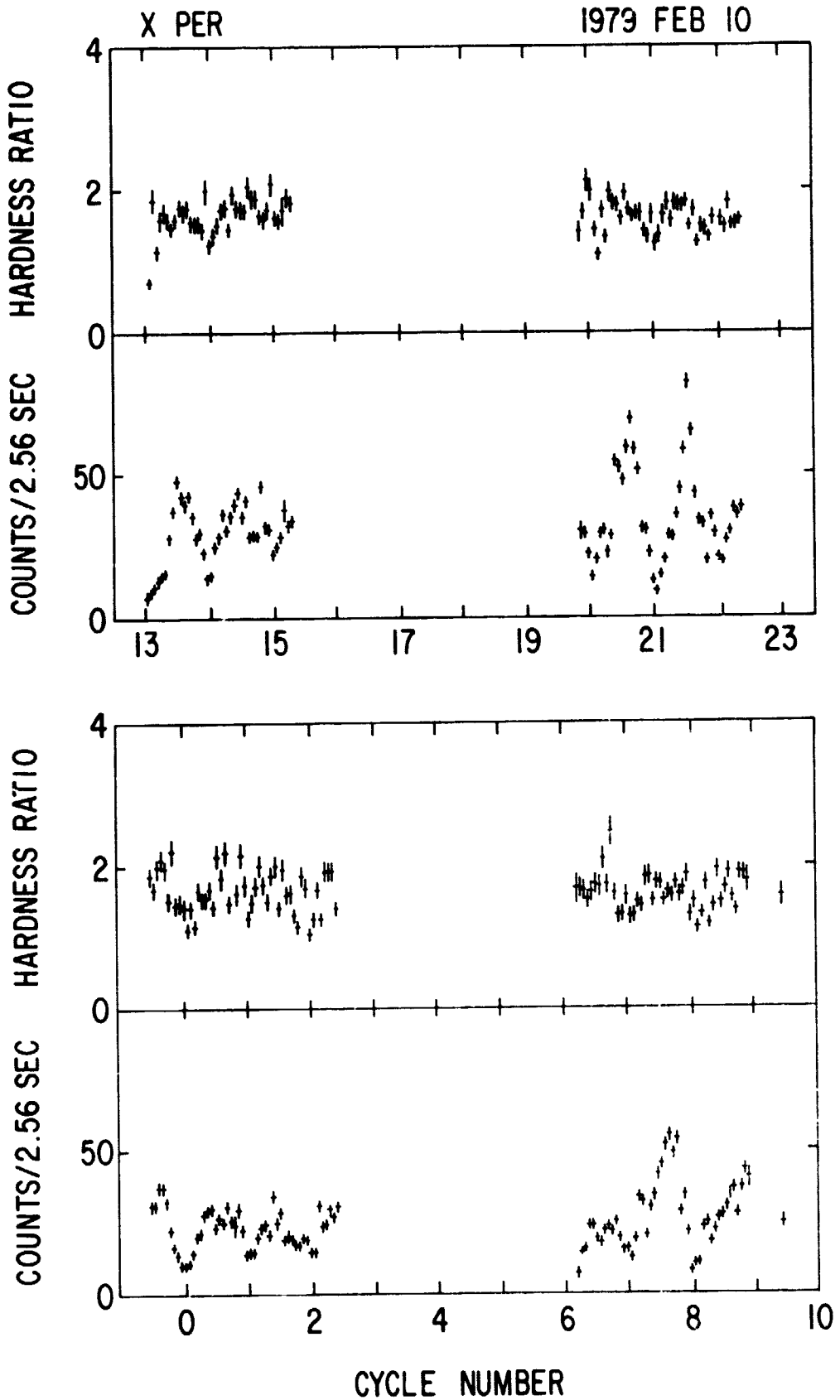


Figure 1

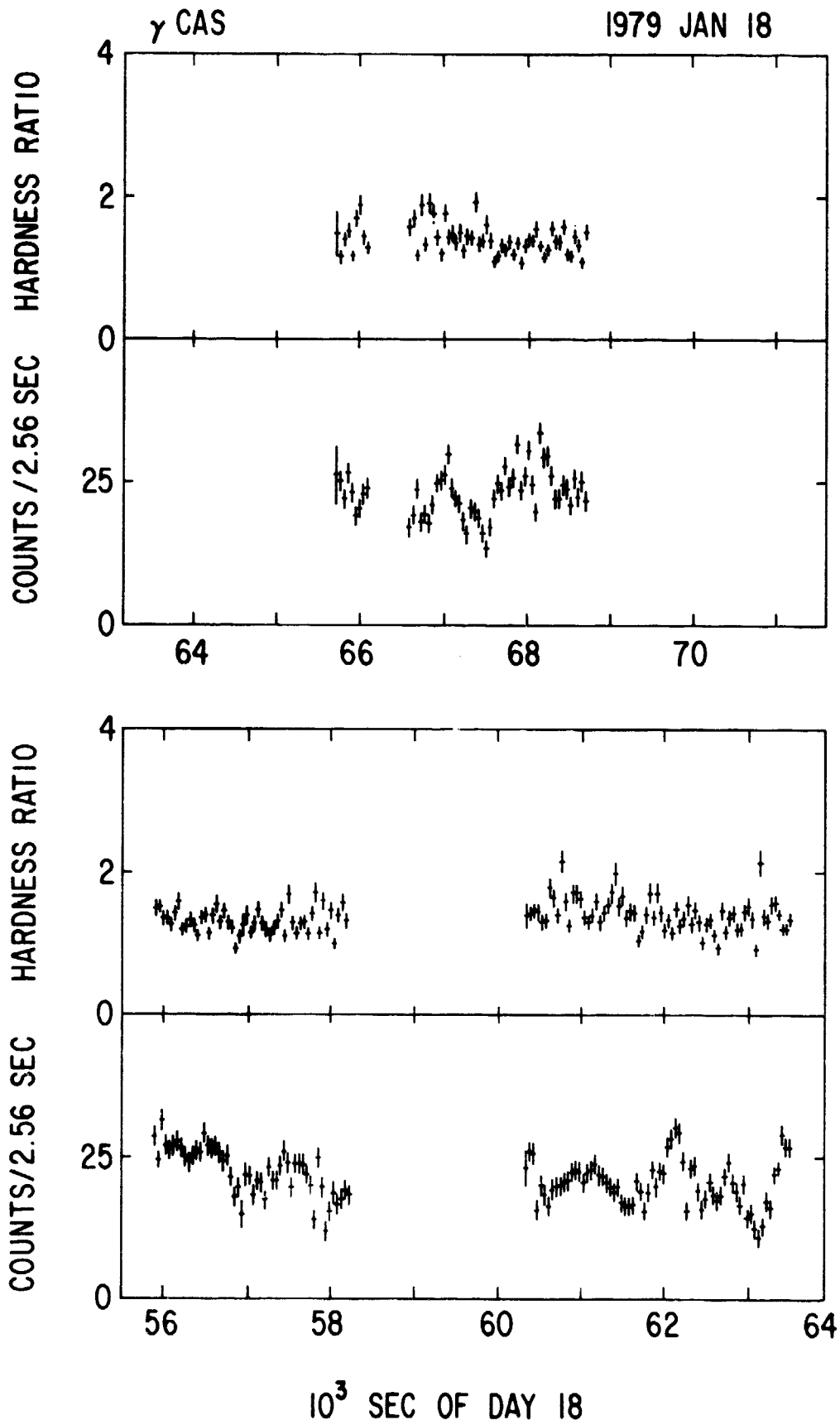


Figure 2

X PER

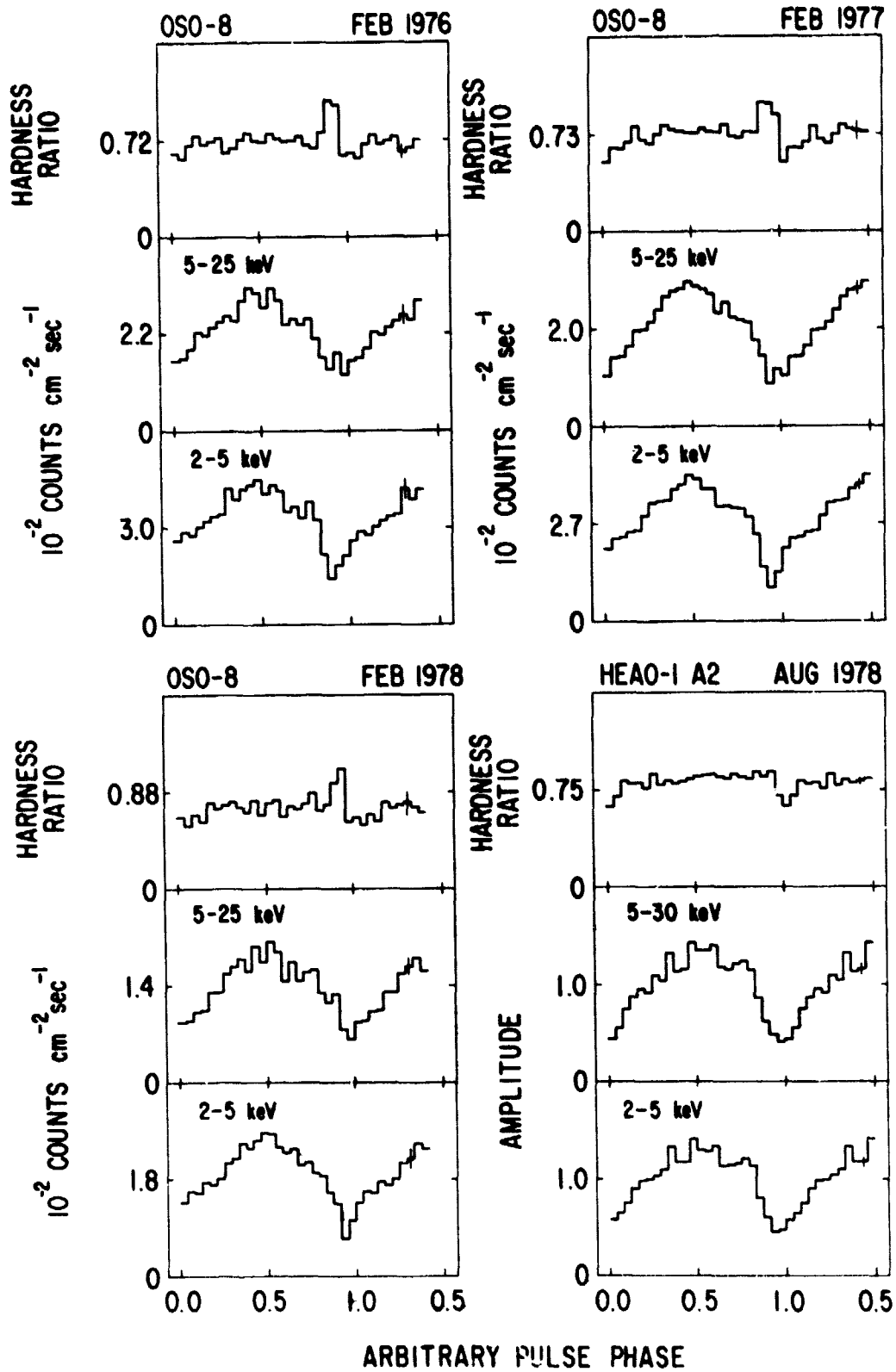


Figure 3

HEAO-1 A2

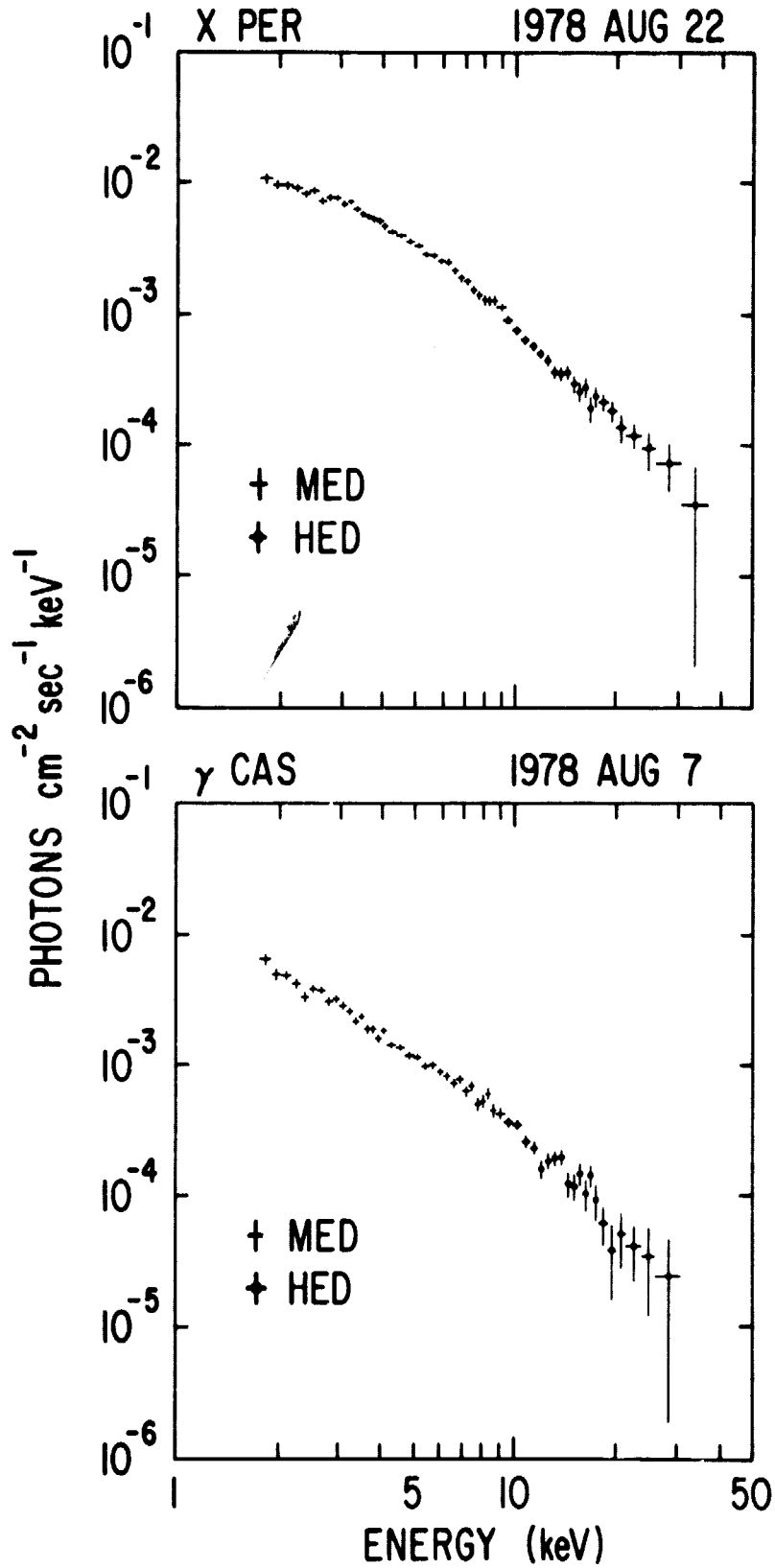


Figure 5

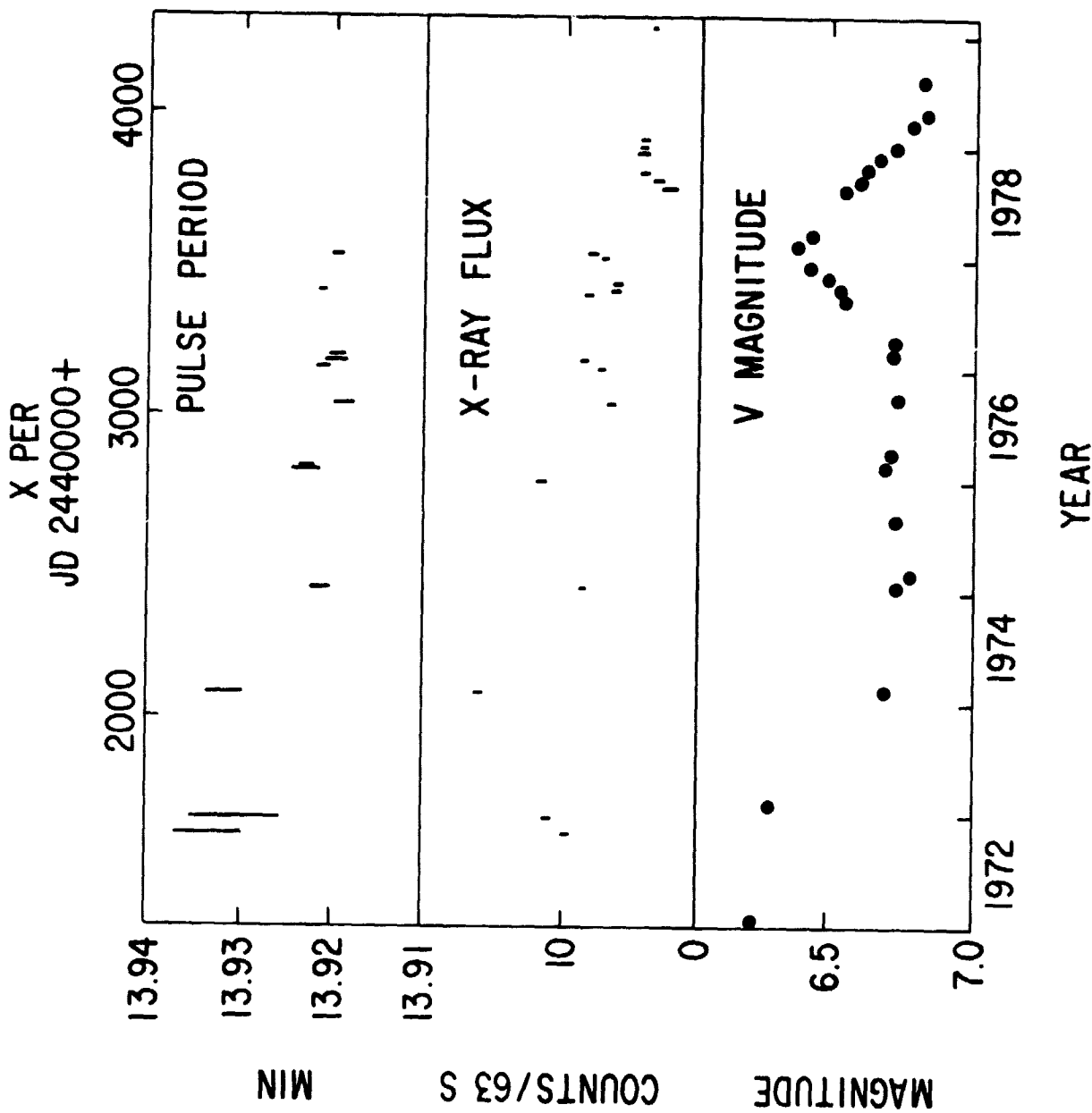


Figure 6

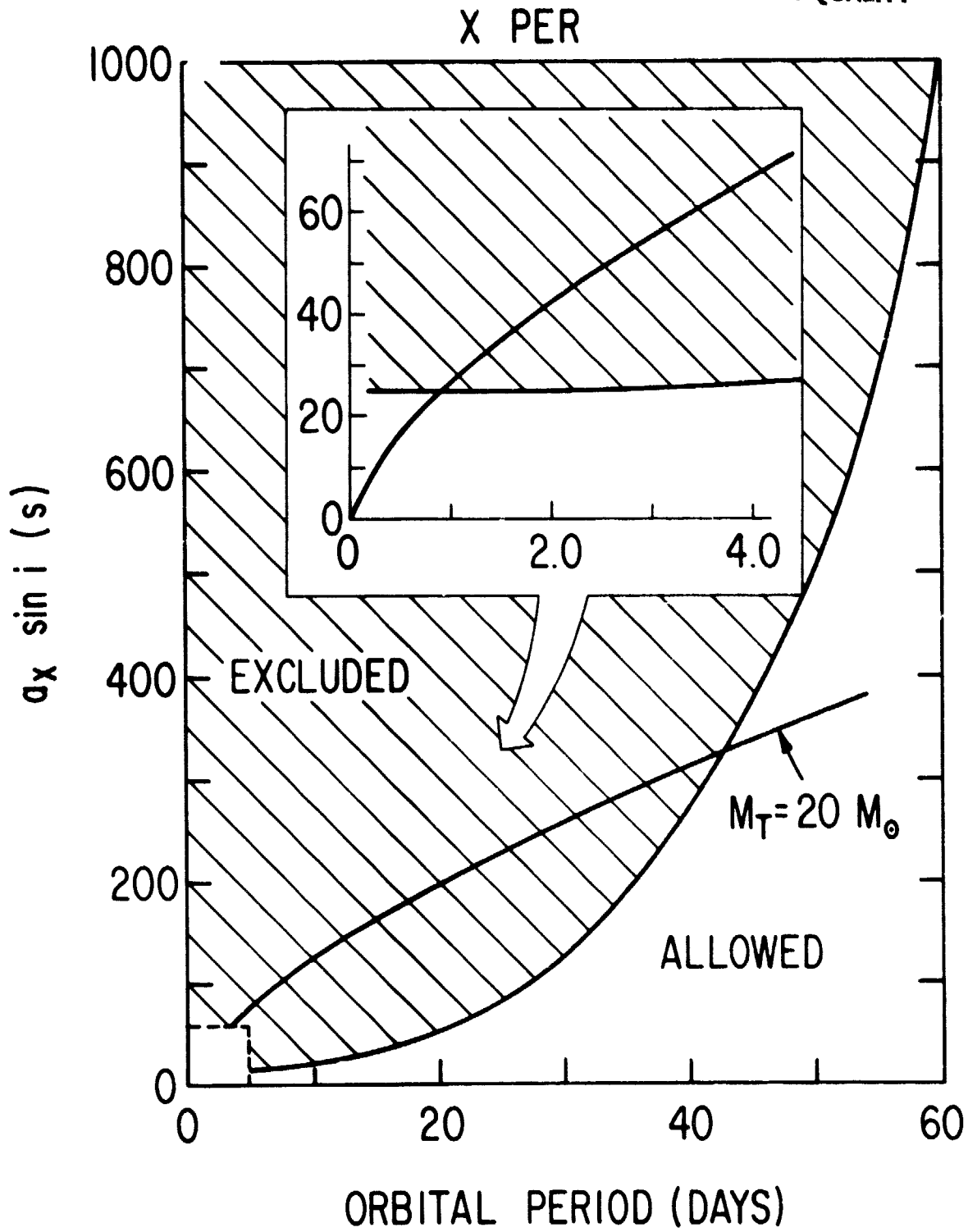


Figure 7